

1 **Supplemental Material for “Biogenic and Biomass Burning Aerosol in a Boreal Forest at**  
2 **Hyytiälä, Finland during HUMPPA-COPEC 2010”**

3  
4 **S.1 Organic Acids Comparison**

5 Correlation between the sum of all functional groups, measured by FTIR, and the sum of all  
6 particle phase organic acids between  $m/z$  100 to 500 (averaged during filter sampling interval),  
7 measured by APCI-MS, is shown in Figure S1. Linear regression results in  $r = 0.90$ , showing a  
8 good agreement between those techniques. The highest AMS O/C ratio of 0.81 was measured on  
9 24 July (FIN 133, filter number), the day with the sole nucleation event of the campaign. Due to  
10 low organic aerosol masses, both instruments measured values close to zero, however, the high  
11 O/C ratio might indicate that organic acids play a key role during nucleation. On the days 29 July  
12 (FIN155), 8 August and 9 August (FIN184, FIN186), when biomass burning aerosol arrived at  
13 Hyytiälä, both instruments show highest signals in mass and FTIR indicates O/C ratios which are  
14 above the campaign average. The correlations between the FTIR and APCI-MS signals were all  
15 quite high, with carboxylic acid functional groups having  $r = 0.84$ , and other corresponding  
16 groups even higher: alcohol (0.86), alkane (0.85), amine (0.88), and carbonyl (0.93) groups.

17  
18 **S.2 Factor Analysis**

19 Positive Matrix Factorization (PMF) was applied to FTIR and AMS spectra to identify robust,  
20 linearly independent components representing local and regional sources of OM. Factor solutions  
21 were analyzed by number of factors, rotational values (FPEAK), and starting seed values. In  
22 depth factor selection criteria are described below for FTIR and AMS factors.

23  
24 **S. 2. 1 FTIR Factor Analysis**

25 PMF was applied to 65 submicron FTIR spectra. The portion of the spectra with quantifiable  
26 peaks ( $3800\text{-}1500\text{ cm}^{-1}$ , with the exclusion of the Teflon interference) was used for the analysis  
27 and the standard deviation of each wavenumber for the back filters was used as the uncertainty  
28 for PMF [Russell *et al.*, 2009]. Robust mode was used and rotational values (FPEAKs) of  $\pm 1.2$ ,  
29  $\pm 1.0$ ,  $\pm 0.8$ ,  $\pm 0.6$ ,  $\pm 0.4$ ,  $\pm 0.2$  and 0 were evaluated. All rotations were examined and it was  
30 observed that FPEAKs  $>0.2$  resulted in unrealistic spectra (i.e. single functional group or lacking  
31 alkane functional group), consistent with *factor splitting* [Ulbrich *et al.*, 2009]. Minimum

1  $Q/Q_{\text{expected}}$ , as described by Paatero et al. [2002], was used for FPEAK selection (Figure S2), and  
2 solutions of FPEAK of 0 were selected. Seed values of 0, 10, and 100 were investigated to check  
3 for robustness of the solutions. Amongst the seed values, correlations ( $r$ ) of the factor spectra  
4 and time series were  $>0.95$ , showing consistency amongst the solutions. A seed value of 0 was  
5 chosen to represent the FTIR solution.

6  
7 A set of solutions, ranging from 2- to 7-factors were examined.  $Q/Q_{\text{expected}}$  decreased with  
8 increasing number of factors in the solution (Figure S3), suggesting a higher number of factors  
9 better fit the observed FTIR spectra. However, solutions with  $> 4$  factors resulted in unrealistic  
10 spectra, which contained no real physical meaning. Additionally, solutions with  $> 4$  factors  
11 generated unidentified factors, small factors ( $< 5\%$  OM), or factors that correlated strongly ( $r >$   
12  $0.65$ ) with respect to time or spectral signature with other factors in the set of solutions, while 2-  
13 and 3-factor solutions underrepresented total OM ( $< 85\%$  OM). The 4-factor solution recreated  
14  $95\%$  of the total OM and generated linearly-independent factors with specific source signatures.

### 15 16 **S.2.2 AMS Factor Analysis**

17 Unit-mass resolution PMF was performed on C-ToF-AMS data. Data and error matrices were  
18 generated using SQUIRREL (version 1.51) with Igor Pro 6.12 (WaveMetrics, Lake Oswego,  
19 OR). The PET software and analysis described by Ulbrich et al. [2009] were used to perform  
20 PMF. Due to low signal to noise (S/N), ion fragments with  $m/z > 100$  were removed from the  
21 analysis. Ion fragments with  $0.2 < S/N < 2$  were downweighted by a factor of 2, in addition the  
22  $\text{CO}_2^+$  ions and their fragments ( $m/z$  16, 17, 18, 28, and 44) were downweighted by a factor of 10  
23 due to the highly oxygenated nature of aerosol at Hyytiälä [Paatero and Hopke, 2003; Ulbrich et  
24 al., 2009]. Additionally,  $m/z$  24 was downweighted by a factor of 10 because of a high sum of  
25 squared residuals observed for this fragment. Robust mode was used and FPEAKs of  $\pm 1.2$ ,  $\pm 1.0$ ,  
26  $\pm 0.8$ ,  $\pm 0.6$ ,  $\pm 0.4$ ,  $\pm 0.2$  and 0 were evaluated.  $Q/Q_{\text{expected}}$  was found to decrease with FPEAK  
27 (Figure S2); however, minimum  $Q/Q_{\text{expected}}$  (FPEAK=0) was not selected for the final solution.  
28 Mathematically ideal solutions (FPEAK=0) are not necessarily the best solution, if the spectra  
29 are unrealistic or have undergone *factor splitting* [Ulbrich et al., 2009]. Solutions for FPEAK  $>$  -  
30 0.4 contained one or more factors that lacked  $m/z$  43 ( $\text{C}_2\text{H}_3\text{O}^+$  and  $\text{C}_3\text{H}_7^+$ ), a predominant  
31 fragment, suggesting the solutions from these rotational values were unrealistic and over split.

1 FPEAK of -0.4 was selected to best represent the solution.

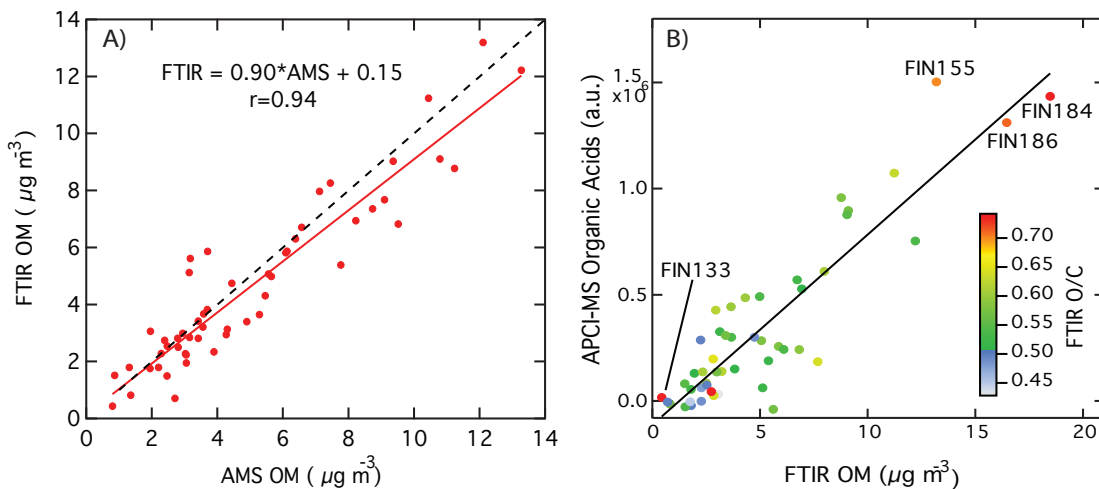
2  
3 Solutions with 2- to 7-factors were analyzed to determine the set of factors that best describe the  
4 measured organic fragments at Hyytiälä. Solutions with  $> 4$  factors resulted in factors that were  
5 small ( $< 7\%$  OM) and were highly correlated in time ( $r > 0.8$ ), indicating some factors had split.  
6 Additionally solutions with 4 or more factors contained factors that lacked  $m/z$  43 or 44 or had  
7 other unrealistic spectra, also suggesting factor splitting. The 2-factor solution was able to  
8 reconstruct 97% of the OM variability, but this was improved by allowing 3 factors, which  
9 reconstructed 100%. The 3-factor solution was found to have factors with substantial masses ( $>$   
10 25% OM) and had strong correlations to organic tracers, in addition to weak temporal  
11 correlations among the factors. For such reasons, the 3-factor solution was chosen to represent  
12 OM components measured at Hyytiälä.

### 14 **S.3 Biogenic and Biomass Burning Separation in FTIR Factors**

15 The three-factor solution contained  $\text{FFC1}_{\text{FTIR}}$ ,  $\text{BIO}_{\text{FTIR}}$ , and  $\text{BB}_{\text{FTIR}}$ , but only explained 85% of  
16 OM variability. However,  $\text{BIO}_{\text{FTIR}}$ , and  $\text{BB}_{\text{FTIR}}$  were similar both temporally and chemically  
17 between the three and four factor split (Figure S6).  $\text{FFC2}_{\text{FTIR}}$  presented only in the four-factor  
18 solution, with the majority of the mass arising from  $\text{FFC1}_{\text{FTIR}}$  and a small fraction evolving from  
19 the  $\text{BIO}_{\text{FTIR}}$  mass in the three-factor solution. Such robustness in the biogenic and biomass  
20 burning factor spectra and profile strength suggests that biogenic and biomass burning aerosol  
21 separated completely, and the factor OM of each source is chemically consistent.

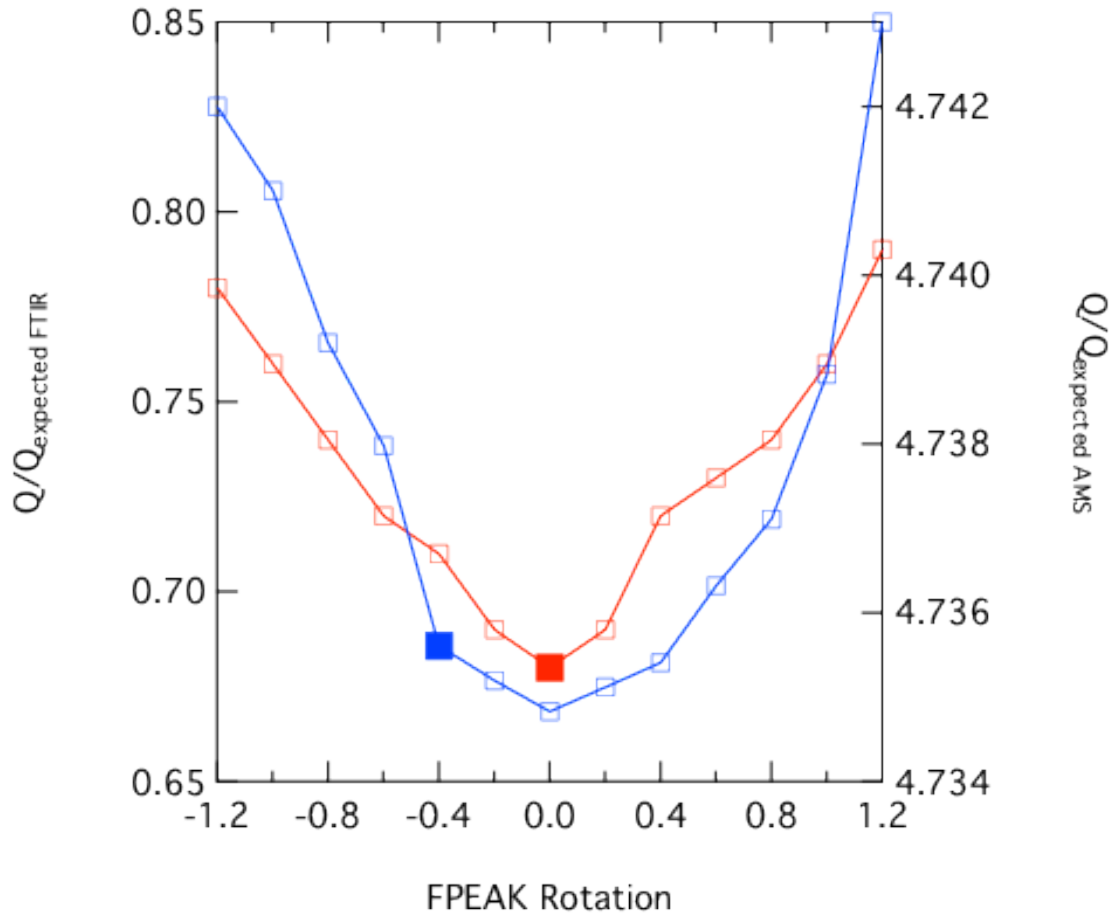
1 **Supplemental Figures**

2 Figure S1 - (a) FTIR OM compared with filter-averaged AMS OM (solid fit line:  $y = 0.9x +$   
3  $0.15$ ,  $r = 0.94$ ). Dashed line represents 1:1. (b) Correlation between FTIR OM and the filter-  
4 averaged sum of all particle-phase signals between  $m/z$  100 to 500 measured by APCI-MS (solid  
5 fit line:  $y = 8.96e+04x - 1.2e+05$ ,  $R = 0.90$ ). Arbitrary units (a.u.) were used for APCI-MS  
6 organic acids.



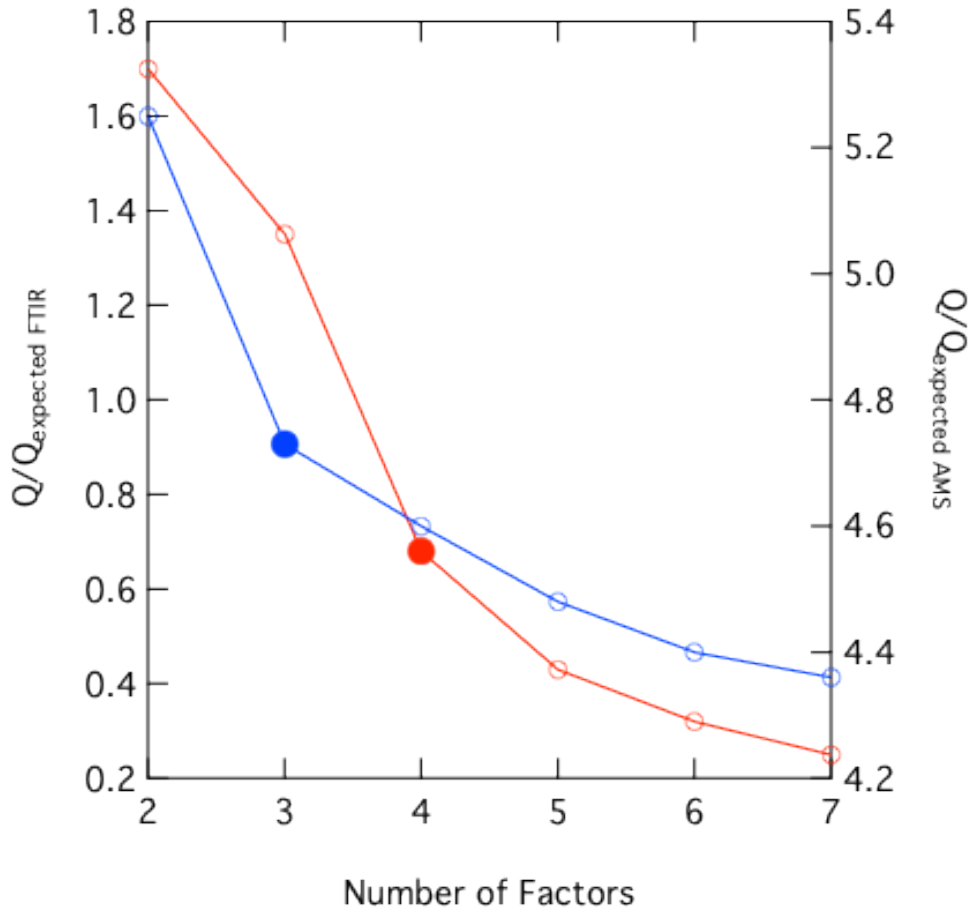
7  
8  
9  
10  
11  
12  
13  
14  
15  
16  
17  
18  
19  
20

1 Figure S2 –Dependence of  $Q/Q_{\text{expected}}$  on FPEAK rotation for FTIR (red, left axis) and AMS  
2 (blue, right axis) factors. Solid squares indicate selected solution for FTIR and AMS factors.  
3



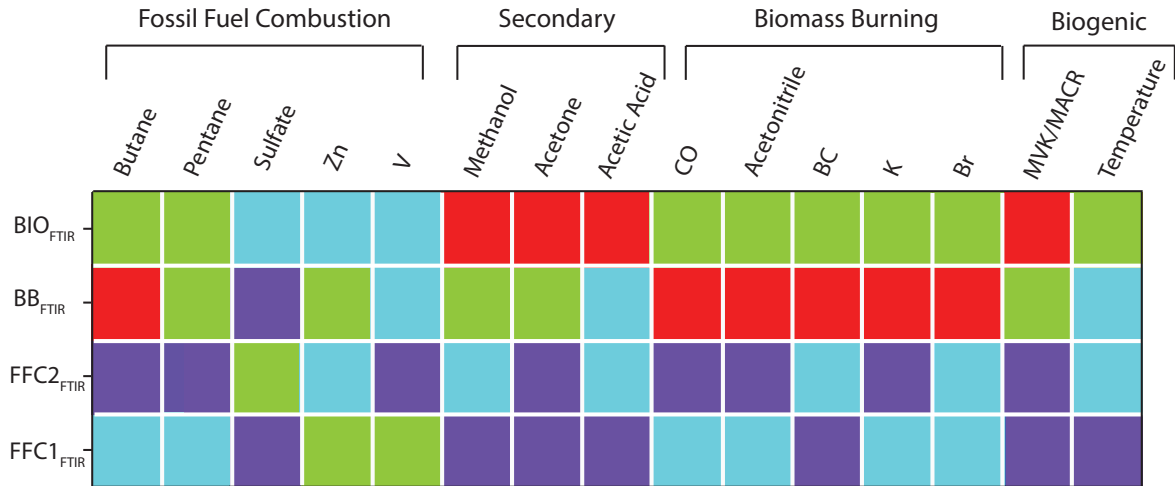
4  
5  
6  
7  
8  
9  
10  
11  
12  
13  
14  
15

1 Figure S3 – Dependence of  $Q/Q_{\text{expected}}$  on number of factors in a set of solutions for FTIR (red,  
2 left axis) and AMS (blue, right axis). Solid circles indicate selected solution for FTIR and AMS  
3 factors.



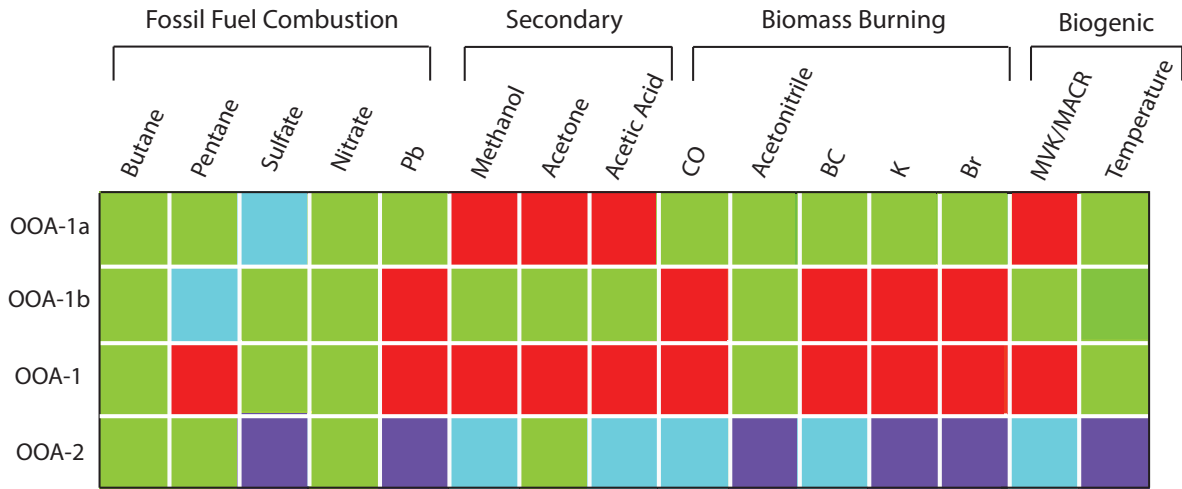
4  
5  
6  
7  
8  
9  
10  
11  
12  
13  
14  
15

1 Figure S4 - Correlations coefficients (r) of FTIR factors and source markers. Colors indicate  
 2 strength of correlation coefficient, strong ( $r > 0.75$ , red), moderate ( $0.5 < r < 0.75$ , green), weak  
 3 ( $0.25 < r < 0.5$ , light blue), no correlation ( $-0.25 < r < 0.25$ , purple).



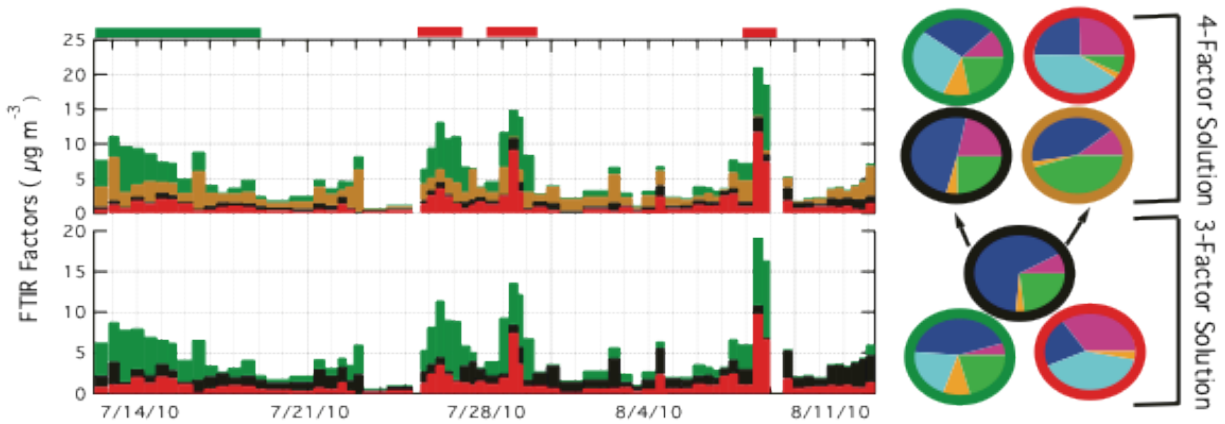
4  
 5  
 6  
 7  
 8  
 9  
 10  
 11  
 12  
 13  
 14  
 15  
 16  
 17  
 18  
 19  
 20  
 21  
 22

1 Figure S5 - Correlations coefficients (r) of AMS factors and source markers. Colors indicate  
 2 strength of correlation coefficient, strong ( $r > 0.75$ , red), moderate ( $0.5 < r < 0.75$ , green), weak  
 3 ( $0.25 < r < 0.5$ , light blue), no correlation ( $-0.25 < r < 0.25$ , purple).



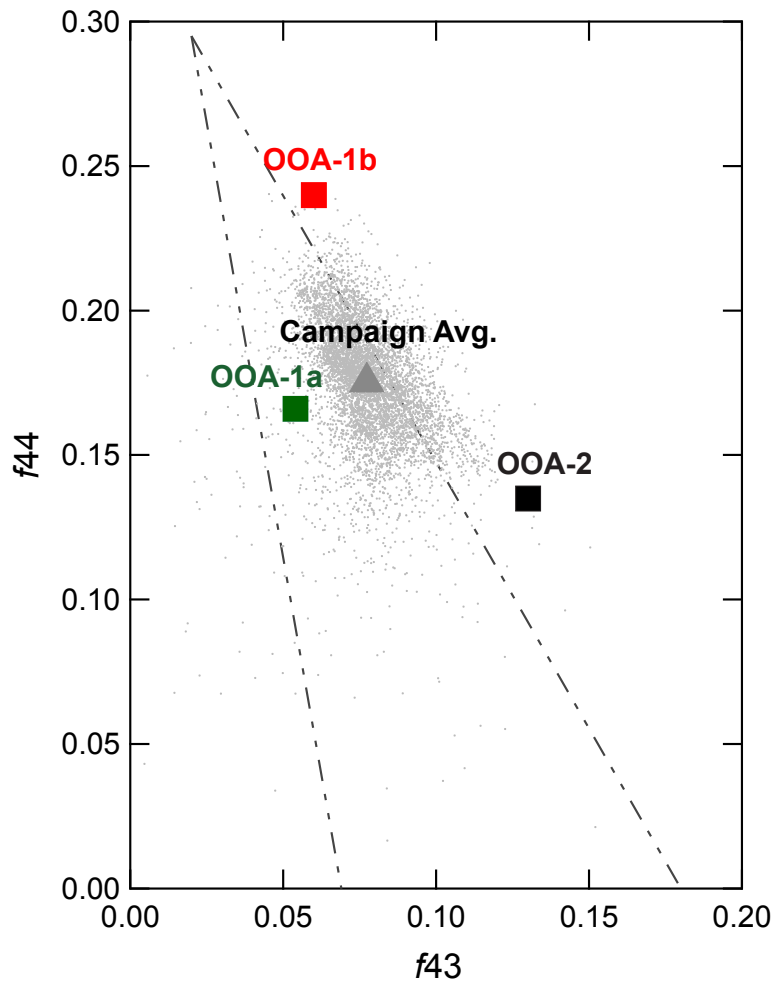
4  
 5  
 6  
 7  
 8  
 9  
 10  
 11  
 12  
 13  
 14  
 15  
 16  
 17  
 18  
 19  
 20  
 21

1 Figure S6 – Time series of submicron OM reconstructed from PMF analysis on FTIR spectra of  
2 the (top) four-factor solution with Combustion 1 (black), Combustion 2 (brown), Biomass  
3 Burning (red), and Biogenics (green) and (bottom) three-factor solution. Arrows indicate split of  
4 Combustion 1 factor between the three-factor and four-factor solution. Color bars on top of  
5 figure indicate periods of stressed boreal conditions (green) and biomass burning (red).



6  
7  
8  
9  
10  
11  
12  
13  
14  
15  
16  
17  
18  
19  
20  
21  
22  
23  
24

1 Figure S7 – C-ToF- AMS organic aerosol composition in the [Ng *et al.*, 2010] triangle space ( $f_{44}$   
2 vs  $f_{43}$ ). Hyytiälä organic aerosol (grey points) fall mostly within Ng triangle space, with bulk  
3 organic aerosol (campaign average: grey triangle) also falling inside triangle space. Factors from  
4 3-factor PMF solution are plotted, OOA-1a (green), OOA-1b (red), and OOA-2 (black).  
5



6  
7  
8  
9  
10  
11  
12  
13  
14  
15  
16

1 **References**

2

3 Ng, N. L., et al. (2010), Organic aerosol components observed in northern hemispheric datasets  
4 from aerosol mass spectrometry, *Atmospheric Chemistry and Physics*, 10(10), 4625-4641.

5 Paatero, P., et al. (2002), Understanding and controlling rotations in factor analytic models,  
6 *Chemometrics and Intelligent Laboratory Systems*, 60(1-2), 253-264.

7 Paatero, P., and P. K. Hopke (2003), Discarding or downweighting high-noise variables in factor  
8 analytic models, *Analytica Chimica Acta*, 490(1-2), 277-289.

9 Russell, L. M., et al. (2009), Oxygenated fraction and mass of organic aerosol from direct  
10 emission and atmospheric processing measured on the r/v ronald brown during  
11 texaqs/gomaccs 2006, *Journal of Geophysical Research-Atmospheres*, 114.

12 Ulbrich, I. M., et al. (2009), Interpretation of organic components from positive matrix  
13 factorization of aerosol mass spectrometric data, *Atmospheric Chemistry and Physics*, 9(9),  
14 2891-2918.

15

16